Sixth International Symposium on Marine Propulsors
smp'19, Rome, Italy, May 2019

On the benefits of metallic additive manufacturing for propellers

Pol Muller[1], Guillaume Rückert[2], Patrice Vinot[2]

[1]SIREHNA, Nantes, France
[2]NAVAL GROUP, Nantes, France

ABSTRACT

While ship propellers have little changed over the past decades, the simultaneous development of advanced numerical simulations and additive manufacturing technology unveils new perspectives. The manufacturing process offers new design freedom with possible improvement of direct and transverse propeller performances such as reduction of mass, reduction of power consumption or better acoustic performances.

Naval Group has very early sensed the advantages of these technologies applied to propellers and decided to work on them. Today, Naval Group has developed a technological expertise all along the process, from the design using numerical tools, through the process simulation, up to the realisation of a demo hollow blade.

This paper focuses on the development of a global numerical tool chain and its application to a hollow propeller concept optimisation, which has later been actually manufactured. The design tools consist of a set of methods and software able to compute propeller performances, automate the design process and achieve better performances with the help of optimisation environments and algorithms.

The application case is a propeller with hollow blades, potentially extremely complex or even impossible to build with a classical foundry process. This paper emphasises the new paradigm that is offered to the designer and how this manufacturing process can contribute to better performances of propellers for the benefits of energy savings, cavitation improvement, and noise and vibrations reduction.

Keywords

Additive manufacturing, WAAM, propeller optimisation, mass reduction.

1 Presentation of the manufacturing process

The manufacturing process consists of a multipass welding using a multiaxial robot solution: the wire deposit in 3D or wire arc additive manufacturing (WAAM). The blade is built layer by layer with a wire fusion by automatic arc welding using a multi-axis robotic arm. Some industrial companies have already applied this technology for 20 years on specific products for different steels. More recently, the possibilities has been shown for WAAM to build a complex design with different alloys, including stainless steel used for naval applications. The present manufacturing process has been developed in the framework of the Joint Laboratory of Marine Technology (JLMT) by Naval Group Research and Ecole Centrale de Nantes. It can be an innovative solution to propose a credible alternative for rough cast parts with a large size and a quite complex geometries such as propellers or propeller blades. The investigations conducted regarding process parameter optimisation associated with metallurgical and mechanical properties have been described in (Queguineur et al 2018).

2 Presentation of the concept

When they are operating behind a ship hull, propeller blades are subject to a non-uniform inflow due to the disturbances induced by the boundary layer of the hull and by the possible presence of appendages such as shafts or brackets. The resulting forces on a marine propeller blade tend to favour bending stresses, with a large alternating loading inducing fatigue. In the blade design phase, the thicknesses are generally defined to ensure the mechanical resistance of the blades in flexion, with fatigue considerations for the maximum speed and power condition, and with static considerations for the dimensioning conditions in manoeuvres (mainly bollard conditions). We do not consider here the specific requirements for ships sailing in ice or polar conditions. Given the mass induced, the blade thicknesses tend to be minimised to match the simple stress criterion, sometimes to the detriment of the hydrodynamic criteria.

The variation of forces on a blade hydrodynamic section during a revolution is in particular due to the angle of attack variation induced by the non-uniform inflow on the section. The hydrodynamic profiles can be individually characterised with respect to cavitation by a Brockett diagram (Figure 1) which represents the cavitating conditions on the profile as a function of the angle of attack and of the cavitation number. During a blade revolution, the immersion and the angle of attack of the section vary continuously, which leads to the operating profile shown in green on Figure 1. Assuming that the section alignment in the flow is already optimum, one of the ways to increase the cavitation margin, or even to suppress it, is to modify the thicknesses of the sections: by increasing it, the margin with respect to sheet cavitation starting at the leading edge increases, but the margin with respect to the bubble cavitation (starting mid-chord) decreases. There is an

optimum for each blade section. The potential increase of the section thickness compared to values commonly used may result in significant increase of blade mass, which has direct consequences on manufacturing cost, and side consequences on ship operation.

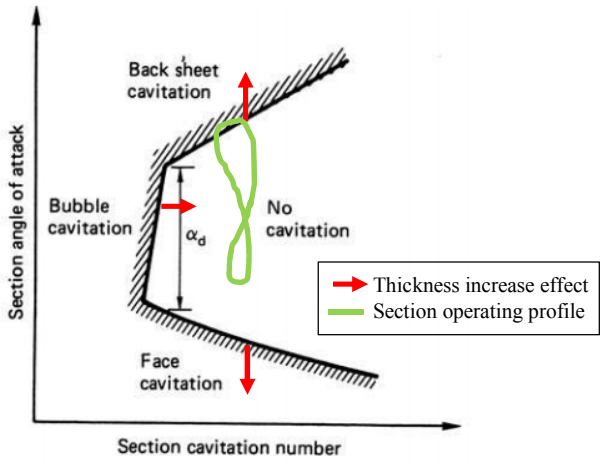

Figure 1: Brockett diagram of a blade section, based on (Carlton 2018)

The concept consists of a propeller with hollow blades, with or without stiffeners. The envelope or wetted part (hereafter denoted as "blade thickness") is defined by an optimum thickness on hydrodynamic criteria without any mechanical or mass consideration, and the wall thicknesses are defined by a mechanical stress analysis. This concept may allow both a mass reduction and an increase in hydrodynamic performance compared to a solid propeller. Although it is potentially extremely complex or even impossible to build with a classical foundry process, the WAAM process offers new possibilities and a new paradigm is offered to the designer in which the balance between weight and hydrodynamic performances is redefined.

Considering that the concept is different from regular propeller blades, the numerical tools which are commonly used in the design phases have to be adapted, but the major gap is on the tools related to the manufacturing process itself.

The design of a hollow blade is made in two sequential phases:

- a first optimisation of the "outer" shape of the blades (wetted surface) dedicated to the enhancement of the hydrodynamic performances,
- a second optimisation of the blade structure (of the cavity) in order to reduce the overall propeller mass, without compromising on blade mechanical strength.

In order to allow the comparison of the performances in particular on the impact of the concept of hollow blade, a reference case has been chosen and most of the geometrical characteristics of the original propeller are preserved: diameter, number of blades, radial distribution of pitch, chord, camber, skew and rake, and family of lifting profiles namely NACA66 with NACA a=0.8 meanline. Only the radial distribution of maximum thickness is modified. The case selected is the KRISO Container Ship (KCS), a container ship widely used as a reference case by the scientific community. Information is available, for example, on the Japanese National Maritime Research Institute (NMRI) website[1].

The main particulars of the propeller, at the service speed of 24 knots, are as follows:

- Wake fraction : 0.227 (measured at a 1:31.6 scale)
- Thrust : 1 940 kN
- Rotation speed : 101.4 RPM
- Delivered power : 27.6 MW
- Diameter : 7.9 m

3 Hydrodynamic design

The impact of the thicknesses is second rank on the hydrodynamic efficiency, assuming that the thickness to chord ratio t/c, also called relative thickness, is in the same order of magnitude as the one of the original blade (no flow separation for instance). The thicknesses of the original blades are defined to meet a criterion of mechanical stresses and it is not envisaged to reduce them. For these reasons, the relative thickness has been set at a maximum of 20% for all dimensionless radii and at a minimum of the ones of the original blade.

The prime objective of the optimisation is to minimise the pressure drops on the blades that is to say to minimise the extension of the cavitation on the blades. This gain makes it possible to limit the noise and vibrations induced by the excessive presence of cavitation, to limit the risk of erosion of the blades or of the rudder, and to limit the radiated noise of the ship, which has a positive impact on the marine fauna and the acoustic stealth of the ship.

Hydrodynamic optimisation uses a calculation chain built specifically for the application case, and automated in order to be integrated in an optimisation environment.

As the incident wake produced by the ship is not uniform (Figure 2), the blade faces a different inflow for each angular position during a complete revolution. Two design conditions are selected corresponding to two angular blade positions less favourable for the pressure fields: the blade position which provides the maximum thrust leads to the largest depression on the suction side, and the blade position which provides the minimum thrust leads to the largest depression on the pressure side. These two conditions are sufficient to determine the most

[1] https://www.nmri.go.jp/institutes/fluid_performance_evaluation/cfd_rd/cfdws05/Detail/KCS/container.html

unfavourable pressures on the entire blade for all the angular positions of the blade.

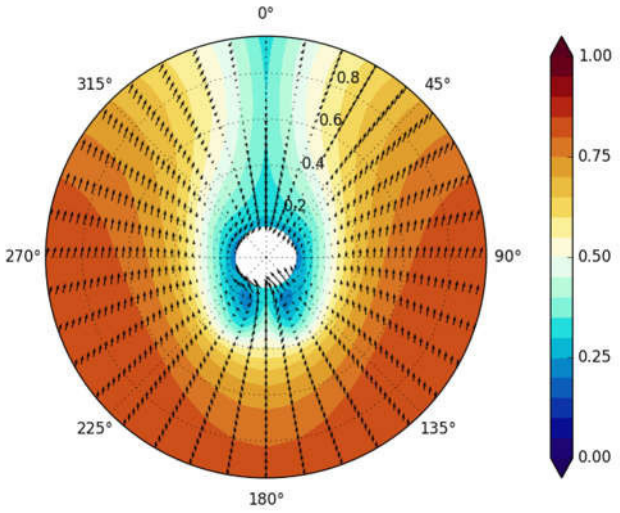

Figure 2: Wakefield map in the KCS propeller plane, as computed using STAR-CCM+ in RANS

The hydrodynamic performance calculations use PROCAL, a potential code developed in the Cooperative Research Ships (CRS) working groups and specially adapted to the calculation of flow on propeller blades. The calculation steps are chained by the ORPHEE 2.0 framework developed by SIREHNA:

- Creation of the geometric file for the meshing tool,
- Propeller mesh,
- Calculation of the pressure field in the blade position which provides the maximum thrust,
- Calculation of the pressure field in the blade position which provides the minimum thrust,
- Calculation of the volume of a blade,
- Extraction of performances in the results files (thrust, torque, efficiency, pressures, etc…).

The calculation chain is built in such a way that the information provided by the user or by the optimisation environment is limited to the parameters of the maximum thickness radial variation curve. In the present case, this curve has been defined by a spline connecting control points.

Geometrical variants are generated using a pseudo-random algorithm (SOBOL) allowing a better coverage of the vector space of the parameters. A set of about 2 000 geometric variants has been computed. For each of these variants, the dimensionless pressure coefficients CP_n were recorded at the same radii as the thickness parameters, for both faces of the blade and for the two loading cases: at the maximum thrust corresponding to the maximum angles of attack on the blades and the strongest depressions on the suction side, and minimum thrust corresponding to the minimum angles of attack on the blades and the strongest depressions on the pressure side. The value of the minimum pressure coefficient CP_n for the set of configurations is computed for each dimensionless radius, and added to the cavitation number σ_n. This magnitude, which we will call "cavitation criterion", directly characterises the risk of cavitation that appears when the magnitude becomes negative. Figure 3 shows examples of results at 0.7R: minimum values of the cavitation criterion as a function of the relative thickness of the section, for all the computed variants.

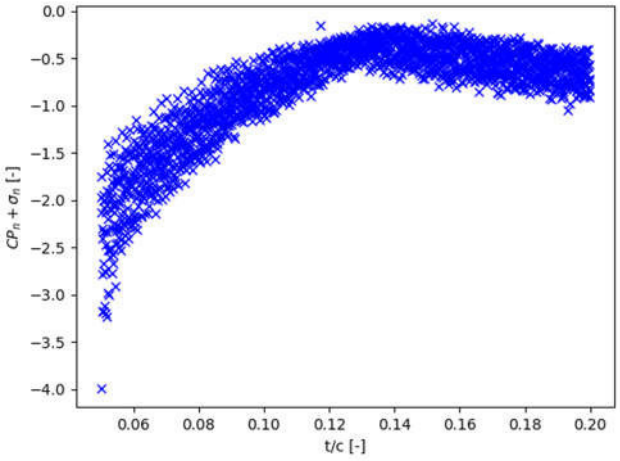

Figure 3: Cavitation criterion as function of the relative thickness at 0.7R

The local minimum pressure is not only dependent on the local thickness but also influenced by the flow in the vicinity, which explains a slight dispersion of the results.

In order to obtain a more global trend and to determine an optimum, a response surface was calculated on the basis of the local average for each relative thickness value (points merged in groups of 1% relative thickness) and each non dimensional radius. The result is presented in Figure 4. The iso-contour of null cavitation criterion has been materialised in bold line (limit of appearance of cavitation): the non-cavitating zone is the one for which the levels are from yellow to green.

It can be seen that for each dimensionless radius of the blade there is an optimum of relative thickness to limit the cavitation extend. This optimum is particularly marked for radii above 0.7R. There is a significant difference between the reference (initial) and optimal thicknesses which results in a large volume of cavitation on the reference blade relative to what could be achieved. At this stage the propeller designer usually has to choose between the cavitation reduction which is achieved by large relative thicknesses, and a reduction of mass which is achieved by reduced relative thicknesses. We can make an intermediate choice considering the possibility of creating a cavity in the blade, which contributes to a mass reduction.

For manufacturing reasons it is not recommended (although not impossible) to increase the absolute thickness towards the tip of the blade. A network of curves has been added to the Figure 4: it represents iso-values of absolute thicknesses. Given the fact that cavitation should not occur for radii lower than 0.6R to 0.65R, the thicknesses in the lower part of the blade remain close to those of the initial blade, while preparing the sharp increase

in relative thicknesses at the blade tip. This increase is made in the area where the risk of cavitation is larger, to approach the optimum, while ensuring to limit the increase in total thickness to the blade tip, so by placing itself close to a iso-contour of total thickness.

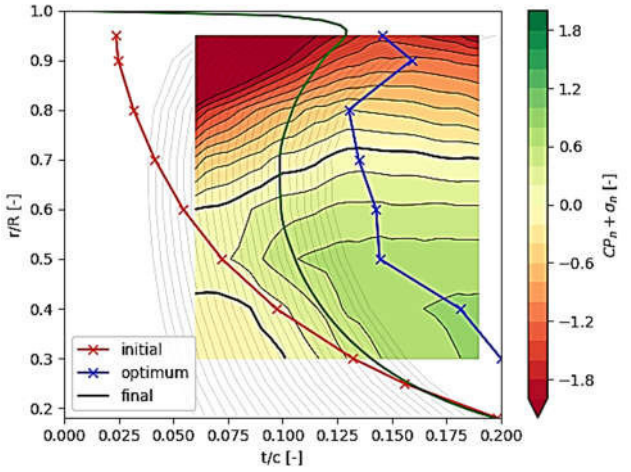

Figure 4: Cavitation criterion as function of the relative thickness for the whole blade

The performances of the reference propeller have been compared to those of the optimised one, for which the radial distribution of thicknesses was modified.

As a first verification step, Figure 5 presents the previously defined cavitation criterion obtained by direct calculation (from the geometry generated, without cavitation), and resulting from the interpolation on the response surface. The error bars correspond to the uncertainty related to the dispersion of the results as presented in Figure 3. There is a very good correlation between the results interpolated and obtained by direct calculation with a slight degradation at the tip of the blade, which strengthens the choice of thickness distribution from the response surface.

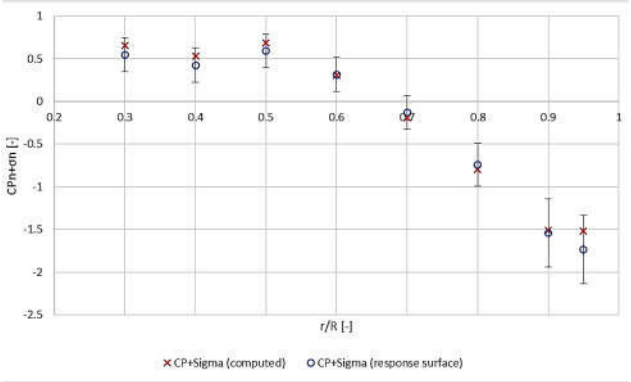

Figure 5 : Comparison of cavitation criterion computed and interpolated

Two performances were then analysed: the propeller efficiency behind the KCS hull and the cavitating regime behaviour in the associated wake (Figure 2).

The calculations use the same software chain as for the optimisation, by adding a calculation in unsteady cavitation regime. The numerical results are shown in Table 1 and views of computed cavitation sheets are shown in Figure 6. In addition views of the pressure distribution along hydrodynamic sections are shown in Figure 8.

Table 1: Comparative performances of the reference and optimised propellers

Quantity	Reference propeller	Optimised propeller	Diff.
Efficiency in behind condition	0.665	0.658	-1.0 %
Maximum proportion of the blade surface covered by cavitation	36.72 %	20.34 %	-44.6 %
Maximum cavitation volume divided by R^3	3.78E-03	1.46E-03	-61.3 %
Variation of the cav. volume divided by R^3 (1^{st} harmonic)	1.63E-03	7.24E-04	-55.7 %
Variation of the cav. volume divided by R^3 (2^{nd} harmonic)	4.41E-04	2.36E-04	-46.5 %
Angular sector where cavitation occurs	168 deg	96 deg	-42.9 %

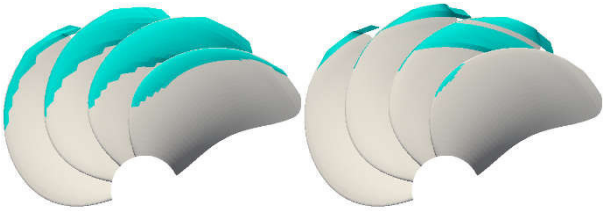

Figure 6 : Overviews of the computed cavitation sheets every 30 deg, left: reference propeller, right: optimised

The reduction of cavitation, both in terms of covered surface and in volume, is very significant, as expected. As presented on Figure 8, the effect of the thickness increase is very significant at the leading edges: the pressure drop is limited by a blunter leading edge, which has a positive impact on the cavitation. On the other hand the pressure is reduced at mid-chord which increases the risk of bubble cavitation. Anyway the pressure at mid chord is still higher than at the leading edge which implies that sheet cavitation will start before bubble cavitation.

The resulting maximum pressure pulses on the hull has been computed by the semi-empirical ETV2 methodology (Empirical Tip Vortex 2), developed by the CRS community. The maximum pressure pulse is 2.7 kPa for the reference blade and 1.6 kPa for the hollow blade. As the exact operating conditions and geometries of the hull have not been taken into account in this computation, results should be taken with caution but clearly indicate a global trend. The same ETV2 methodology gives an estimate of the underwater radiated noise. The results show that the hollow blade reduces the third octave band radiated noise by roughly 5 dB compared to the reference blade in the higher frequencies (> 1 kHz) whereas the noise is increased by roughly 5 dB for the lower frequencies (< 100 Hz). These results should again be considered with caution.

The efficiency of the propeller is very slightly reduced. However, on the one hand the variation calculated here is of the same order of magnitude as the numerical accuracy of the method, and on the other hand all the other

geometrical characteristics of the blade are kept invariant. As that the cavitation volume is significantly reduced by the optimisation, a slight decrease in the blade area ratio (surface of the blades) would allow a first rank gain in efficiency, while maintaining a cavitation volume much lower than what is generated by the reference propeller. It is possible to consider reducing more significantly the surface of the blades to increase the efficiency of the propeller, without degrading the cavitation regime relative to the reference propeller. As a quick estimation of the achievable efficiency increase, the chords of the hollow blade have been reduced in order to produce as much cavitation as the reference blade. This would allow an increase of efficiency in the order of 5%.

The extra thicknesses therefore allow a gain in performance, either on the volume of cavitation generated, or on the efficiency of the propeller (while also reducing the surface of the blades), or both.

4 Mechanical design

The purpose of the mechanical design is to build a cavity as large as possible, in order to reduce the overall blade mass and to cope with the mechanical stresses.

The level and location of the maximum stress on the blade when it is subjected to hydrodynamic loading are evaluated with a stress calculation. The open source finite element code Code_Aster is used in static linear condition, applying the pressure field defined at the hydrodynamic design step, the hydrostatic pressure and the centrifugal forces. In order to modify the blade mass, the radial distribution of wall thickness is modified. In practice, it is defined by an interpolation between three points:

- t_1: the wall thickness at the blade root, varying between 10 mm and 30% of the blade total thickness,
- t_2: the wall thickness at the radius R=0.7, varying between 10 mm and 30% of the blade total thickness,
- r_3 : a fixed wall thickness of 20 mm is imposed at the radius r/R=r_3 (varying between 0.90 and 0.95)

The minimum thickness of 10 mm has been set in accordance with the manufacturing process. Although it could produce much thinner profiles, this value allows to use a similar deposit strategy for any part of the propeller blade, from root to tip.

The calculation process is as follows:

- Choice of the parameters values,
- Construction of the radial distribution of wall thickness,
- Definition of the cavity using parametric CAD software suite CAESES,
- Export of the cavity in CAD format (STEP),
- Generation of the volume mesh based on the outer blade shape (fixed after hydrodynamic optimisation) and the inner cavity shape,
- Finite Element calculation using Code_Aster,
- Post-processing using Paraview (stresses are computed at the Gauss points).

The main parameters of the mechanical calculation model are the material properties, which are as follows.

For the reference blade, in copper alloy:

- Volume mass $\rho_s = 7600 kg/m^3$
- Poisson's ratio $\nu = 0.3$
- Young's modulus $E = 1.25\ 10^{11} Pa$

For the hollow blade, in duplex steel:

- Volume mass $\rho_s = 7850 kg/m^3$
- Poisson's ratio $\nu = 0.3$
- Young's modulus $E = 2.1\ 10^{11} Pa$

The difference in material produces differences in stresses as will be presented later but one should focus on the ratio between actual stresses and maximum allowable stresses. In this case the difference in material is not the root cause of the differences in performances.

As detailed previously the blade is subject to an unsteady pressure field during a revolution which leads to alternating stresses. During the life of the propeller, the number of cycles is high, well above 1.10^8. In the present case the loading during a rotation varies of the order of +/-60% of the average loading. It can be shown from a Goodman or a Haigh diagram that the acceptable stress limit taking into account the fatigue behaviour is equivalent to a static stress computed using the average blade loading. For the present case where the material is stainless steel, this equivalent static limit has been fixed to the endurance limit of the material (200 MPa), which is a conservative option. In addition, as the cavity will not be machined after its closure, a safety factor of 1.5 on the stress limit is applied, which leads to a maximum equivalent static stress of 126 MPa. This value will be used as the acceptable stress limit criterion. One can note that this limit is well below the ultimate tensile strength of the material.

No equivalent criterion has been found to the reference blade nevertheless we can make assumptions. The Cu grade 3 bronze properties as suggested by Bureau Veritas rules for classification of steel ships give a tensile strength of 590 MPa and specify that the maximum allowable stress should provide a safety factor of 9 with respect to this limit. This gives a maximum allowable stress of 65 MPa for the reference blade.

A DOE (design of experiment) was carried out in order to scan a set of values of the three cavity parameters. For the computed variants, the extreme radius parameter of the cavity has very little influence on the stresses (parameter r_3).

It is observed that certain radii require significant wall thicknesses to obtain acceptable stresses. Two areas are particularly affected: radii between 0.4 and 0.5R at the trailing edge and between 0.8 and 0.9R at the leading edge. The stresses of the hollow blade on Figure 9 illustrate the phenomenon: in these two areas the maximum stress is

reached at the junction of the walls. Significant fillets have therefore been used to reduce stress concentrations in these areas.

Amongst the variants calculated, the final selection has a wall thickness of 115 mm at the root and 30 mm at 0.7 R. It offers a good compromise between reduction of mass and limitation of the mechanical stresses.

Views of the mechanical stresses and displacements are shown respectively in Figure 9 and Figure 10 for both the reference blade and the hollow blade.

The maximum stress level is in the order of 60 to 65 MPa for the reference blade and 115 to 120 MPa for the hollow blade. Both are in good agreement with the required maximum allowable stress (65 MPa and 126 MPa respectively).

The location of the maximum stress is quite different: for the reference blade there is some stress concentration at the trailing edge, mid span and at the blade root, mid chord. These two locations are quite common for conventional blades. On the other hand, for the hollow blade the maximum stresses are at the junction of the blade walls, at the leading and trailing edges, which is of course not possible for conventional solid blades.

The maximum displacements at the tip of the blades are in the same order of magnitude for both blades: 16 mm for the reference blade and 13 mm for the hollow one (i.e. less than 0.5% of the blade radius in both cases).

The displacement field is also quite different for both blades: for the reference blade the displacement is almost proportional to the local blade radius which is expected for a global bending, whereas one can clearly see the influence of the cavity on the hollow blade. The displacement map of the hollow blade is a superimposition of a global bending similar to the reference blade, and of a local compression of the cavity. Nevertheless this compression is quite small in terms of displacement (maximum 5 mm roughly).

5 Mass reduction

Due to the thickness optimisation, the hollow blade has a significantly higher outer volume than the reference blade (+62.9%) but a cavity has been arranged in this large volume. The resulting mass is reduced by 22.7% even if the volume mass of the alloy used for the hollow blade is higher than the one of the reference blade. Considering that the buoyancy is proportional to the wetted volume, the resulting apparent mass in sea water is even more reduced: 35.6%.

Table 2: Comparison of blade masses

	Reference blade	Hollow blade	Diff.
Blade external volume [m^3]	1.023	1.666	+62.9%
Blade cavity volume [m^3]	0	0.876	-
Mass of one blade [kg]	8030	6209	-22.7%
Apparent mass in sea water [kg]	6980	4498	-35.6%

6 Blade manufacturing

The blade manufacturing process is not the main topic of this paper but the authors want to emphasise that a demonstrator blade has been produced in accordance with the hollow blade design, except for the root attachment which has been simplified (flat plate and not actual hub). As can be seen on Figure 7, the blade is built in successive layers including the cavity. After roughly one third of the total span, the blade has been tilted in order to avoid difficulties at the trailing edge, where the local skew angle is higher that the limit allowed by the process. This can be seen on the right side of the Figure 7 where there is a discontinuity in the material layers. Of course a final machining should be performed as this raw part has a surface roughness which is not compatible with standard requirements.

Figure 7: View of the hollow blade during manufacturing and once completed (not machined)

7 Conclusion and perspectives

The hollow blade provides significant improvement of the hydrodynamic and transverse performances: on the one hand the cavitation is significantly reduced compared to the reference propeller, thanks to a large increase of the blade thickness, and on the other hand the mass is reduced by 23% in air and 36% in water.

These improvements come with no or little impact on the efficiency (the difference is in the same order of magnitude as the accuracy of the numerical method) and with sufficient safety factor against material fatigue.

Side performances which have been presented, such as underwater radiated noise or pressure pulses generated on the ship hull, would need extra investigation for final conclusions. Anyway, with some assumptions and empirical methods, it has been demonstrated that the hollow propeller reduces pressure pulses thanks to a massive reduction of the cavitation volume, and also reduces the underwater radiated noise at higher frequencies where cavitation is the main contributor.

The hollow blade design has been driven by as little modifications as possible to the original blade design,

modifying only the thickness distribution which is usually a consequence of blade strength requirements. Further modifications of the design could increase hydrodynamic performances such as efficiency, using the extra margins against cavitation that have been achieved.

This comparative analysis of the reference and hollow propellers show that the new design capabilities offered by the additive manufacturing process can be used to enhance global propeller performances. This should be taken into account to define new propeller concepts with more freedom than what is imposed by traditional foundry processes.

An evolution of this concept could be a variation of the wall thickness along the blade sections or the use of inner stiffeners since the maximum stresses are localised at the junction of the walls. Both concepts should provide an extra mass reduction.

Several mechanical design points have not been addressed here. A specific point concerns the resistance to the impacts related to objects at sea. These impacts are likely to appear at the leading edge (sailing forward), or trailing edge (sailing backwards) or at the blade tip. By construction these areas are massive and similar to those that would be observed on a full blade. Further validation of good impact resistance could be obtained by following an equivalent of the recommendations of the ship classification rules for polar ice navigation for instance.

Acknowledgment

These developments have been made in the WP11 of the RAMSSES project funded by the European Union's Horizon 2020 research and innovation programme under grant agreement No 723246.

REFERENCES

Carlton, J. (2018). 'Marine propellers and propulsion' Butterworth-Heinemann.

Queguineur, A., Rückert, G., Cortial, F., & Hascoët, J. Y. (2018). 'Evaluation of wire arc additive manufacturing for large-sized components in naval applications' Welding in the World, 62(2), 259-266.

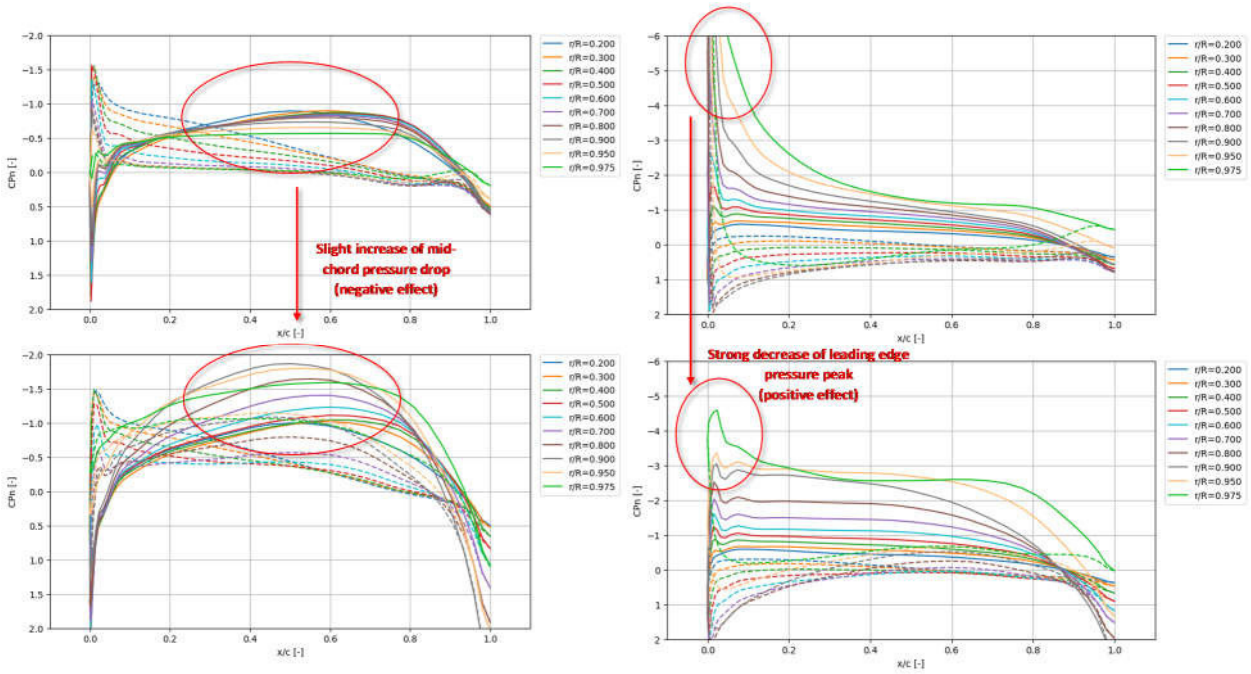

Figure 8: Pressure distribution on the blade sections – top: reference blade, bottom: hollow blade, left: minimum thrust position, right: maximum thrust position (continuous line: suction side, dashed line: pressure side)

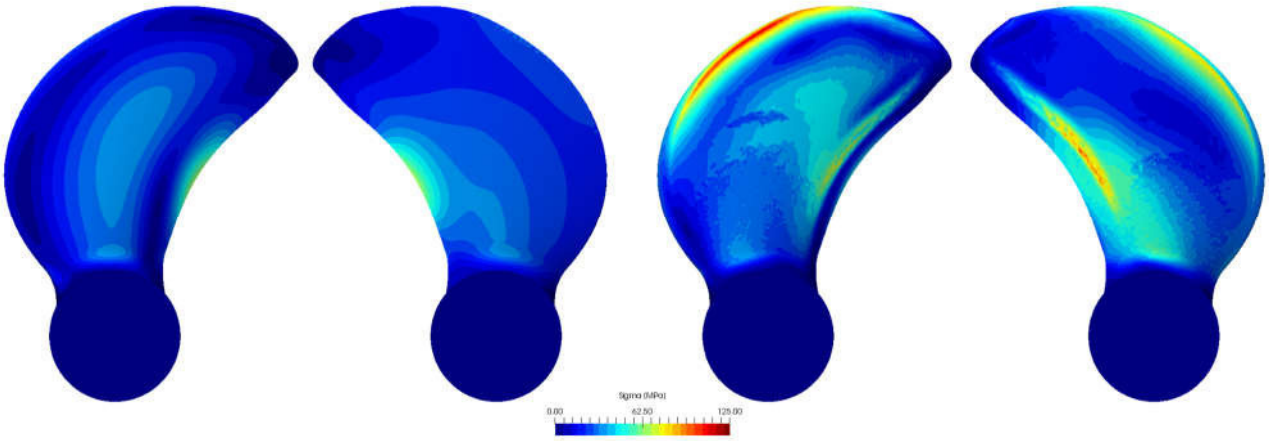

Figure 9: Von Mises stresses on the suction and pressure sides - left: reference blade, right: hollow blade

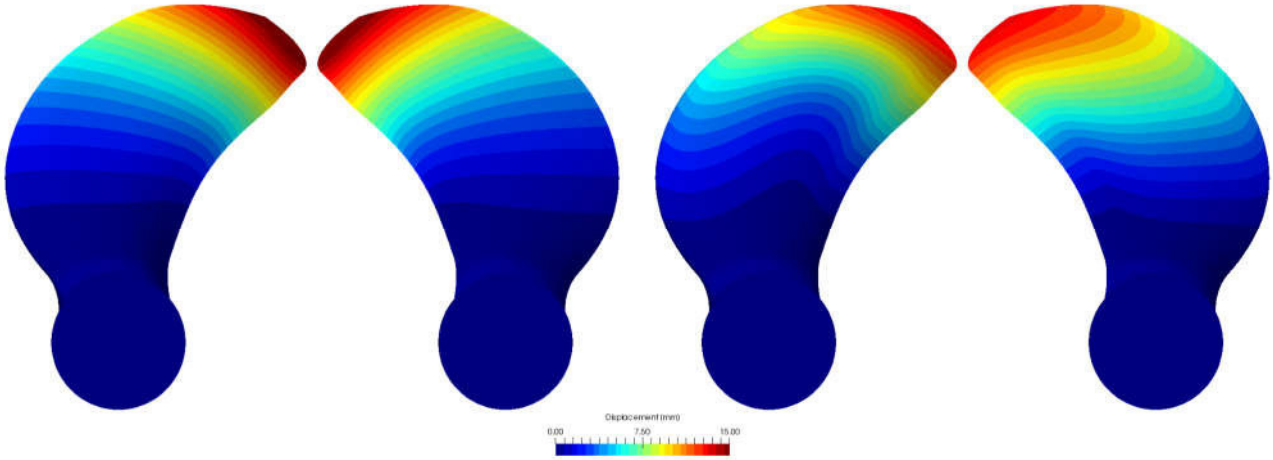

Figure 10: Displacements on the suction and pressure sides - left: reference blade, right: hollow blade